



Comparison of different fittings of experimental DSD

[E. Adirosi](#), [L. Baldini](#), [F. Lombardo](#), [F. Russo](#), and [F. Napolitano](#)

Citation: [AIP Conference Proceedings](#) **1558**, 1669 (2013); doi: 10.1063/1.4825850

View online: <http://dx.doi.org/10.1063/1.4825850>

View Table of Contents: <http://scitation.aip.org/content/aip/proceeding/aipcp/1558?ver=pdfcov>

Published by the [AIP Publishing](#)

Comparison of Different Fittings of Experimental DSD

E. Adirosi^{a,b}, L. Baldini^a, F. Lombardo^c, F. Russo^b and F. Napolitano^b

^a*Istituto di Scienze dell'Atmosfera e del Clima, Consiglio Nazionale delle Ricerche,
Via del Fosso del Cavaliere 100, 00133 Rome, Italy, elisa.adirosi@artov.isac.cnr.it*

^b*Dipartimento di Ingegneria Civile, Edile e Ambientale, Sapienza Università di Roma,
Via Eudossiana 18, 00184 Rome, Italy*

^c*Dipartimento di Ingegneria, Università degli Studi Roma Tre,
Via Vito Volterra 62, 00146 Rome, Italy*

Abstract. Retrieval of a distribution of raindrop sizes from measured drop spectra is critically influenced by the tail of the distribution. The influence of various tail-types is studied with reference to four parameterisations fitted both to the large drops and to the entire sample of the disdrometer-measured spectra. Results of this preliminary analysis show that the Weibull distribution with a shape parameter greater than one seems to fit the highest percentages of the measured drop spectra.

Keywords: Rainfall, Drop Size Distribution, Upper tail, Disdrometer.

PACS: 47.55.D-, 92.40.Ea, 02.50.-r, 92.60.Jq

INTRODUCTION

The knowledge of drop size distribution (DSD) of rain, namely the frequency distribution of drop equivalent diameters has a wide range of applications in earth sciences such as precipitation physics, hydrology and agricultural and soil sciences. DSD is also important in precipitation remote sensing, especially in radar meteorology for relationships among rainfall rate and radar measurements such as the radar reflectivity factor. DSD is the result of different physical processes, such as coalescence, aggregation and breakup involved in the formation and evolution of rain. Consequently, DSD is characterised by a great variability both in space and time. DSD can be defined as

$$N(D) = n_c f_D(D) \quad (1)$$

where n_c is the raindrop concentration (i.e. the zeroth moment of DSD), and $f_D(D)$ is a probability density function (pdf). Various pdfs have been proposed in the literature, such as Exponential [1], Weibull [2], Lognormal [3], and Gamma [4], assuming that a parametric form can describe DSD variability. To date, the commonly most used distribution is the three-parameter gamma [4], usually written as

$$N(D) = N_0 \exp(-AD) D^\mu \quad (2)$$

where N_0 ($\text{mm}^{-1} \text{m}^{-3}$), μ and A (mm^{-1}) are called intercept, shape, and slope parameter, respectively. A common technique for deriving the three parameters from drops spectra collected by a disdrometer is the method of moments, consisting of equating sample moments with unobservable population moments and then solving those equations for the parameters of (2) to be estimated. To accomplish this aim, different sets of raw moments have been proposed (e.g., [5] used the third, fourth, and sixth moments, MM346, whereas [6] considered the zeroth, first and second moments, MM012, which usually perform better than the former in parameter estimation) depending also on the relevance of a moment for a specific application (for example, the second moment is relevant for visibility study, the liquid water content is given by the third moment and is relevant to the attenuation of telecommunication links, the sixth moment is proportional to the reflectivity factor and plays a central role in the radar meteorology, etc.). However, the method of moments can determine an excessive and somehow unrealistic variability of the retrieved parameters [7].

In general, retrieval of parametric DSDs would aim to best model the largest portion of drop spectra with a single f_D . As a consequence, there is no guarantee that the selected distribution will adequately model some DSD portions, such as the tail. For characterising physical quantities such as the liquid water content and radar reflectivity which, respectively, depend on D^3 and D^6 , the right tail is critical because large drops play a much more important role than small droplets. Very large drops (say $D > 5$ mm in diameter) occur quite rarely but can be significant during the very early stage of convective rainfall where a low number of large drops can be recorded [8]. Despite usually occurring drop breaks for large diameters ($D \geq 8$ mm) [9], the most popular DSD models existing in the literature, such as (2), have no upper limit.

To investigate possible limitations in modelling DSD with a single function, we fit the following four different one-sided continuous distributions to the 1-min measured spectra: the Pareto, the Lognormal, the Gamma and the Weibull distributions. The fittings are performed both on the tail of the spectrum only and on the whole spectrum.

EXPERIMENTAL DATASET

Observational data consist of 1-min spectra collected by a two-dimensional video disdrometer (2DVD) during the first special observation period of the hydrological cycle in the Mediterranean experiment (HyMeX) field campaign in Rome from September to November, 2012. The 2DVD is an optical device that measures the equivalent diameter (D in mm), the volume, the fall speed, the axis ratio and the cross-sectional area of each drop that falls in the virtual measuring area of $10 \times 10 \text{ cm}^2$ [10]. From these measurements the empirical DSD is typically obtained by partitioning observed diameters D into 50 bins with a constant width, as

$$N(D_i) = \frac{1}{\Delta t \Delta D} \sum_{k=1}^{M_i} \frac{1}{A_k v_k} \quad (3)$$

where the time span Δt (s) is 60 s, the width of the bin ΔD (mm) is 0.2 mm, the terminal fall velocity v_k (mms^{-1}) is given by [11], M_i is the total number of drops in the i -bin and A_k is the cross sectional area (m^2). To remove the spurious drops due to splashing or wind effect the filter criterion of [12] was adopted, while we assumed a threshold equal to 10 drops to identify a rainy minute.

FITTING METHOD

DSDs were studied subdividing spectra into sectors based on thresholds such as small drops ($D < 1 \text{ mm}$), midsize drops ($1 \text{ mm} < D < 3 \text{ mm}$) and large drops ($D > 3 \text{ mm}$) [8]. We identify the upper part of each spectrum with a $D_{threshold}$, which is defined to be the 90th percentile of drop diameters of hydrometeors measured in a given minute. Consequently, the upper part of the DSD is $N(D \geq D_{threshold})$. To assure an adequate sample size of large drops, only spectra with a minimum 100 drops in total and at least one drop with diameter greater than 3.5 mm are retained, obtaining 485 1-min spectra.

Once the $D_{threshold}$ is set, the distribution fitting requires the minimisation of the modified mean square error (MSE) norm $N1$ defined as [13]:

$$N1 = \frac{1}{N} \sum_{i=n-N+1}^n \left(\frac{F_T(D_i)}{F_E(D_i)} - 1 \right)^2 \quad (4)$$

where, if the fit is performed only on the upper part of the distribution, N is the number of drops with $D \geq D_{threshold}$, otherwise $N=n$ is the total number of drops; $F_T(D_i)$ and $F_E(D_i)$ are the theoretical and the empirical exceedance probability functions (EPFs), respectively, computed for each single drop measured in a given minute. To estimate the $F_E(D_i)$, first the EPF

$$\overline{F}_E(X_i) = 1 - \sum_{i=1}^n \frac{X_i}{n_c} \quad (5)$$

$$X_i = \frac{1}{A_i \Delta t v(D_i)} \quad (6)$$

is computed; since the variable X is inversely proportional to D , then the $\overline{F}_E(D_i) = 1 - \overline{F}_E(X_i)$. The $\overline{F}_T(D_i)$ was computed considering the four different distributions described above [13]. The Pareto is the distribution with the heaviest tail, while the Weibull with shape parameter > 1 is the one with the lightest tail [14]. The practical implication of a light tail is that it predicts less frequent larger drops compared to heavier tails. All the distributions are expressed as a function of two parameters: the scale parameter (β) and the shape parameter (γ). The proposed approach allows fitting of the theoretical distribution only to the largest drops of each spectrum. The fitted distribution would thus provide the best possible description of the tail. The norm $N1$ (4) considers the relative error between the theoretical and empirical values, consequently the advantage of $N1$ over classical square error norms is the ability to properly “weights” each values of the sum. In Sect. 6 of [13], there is a comprehensive analysis regarding the performance of $N1$ and the comparison of the latter with the commonly used norms; the authors believe that the classical norms are more sensible to the contribution of the extreme values, and this behaviour can affect the fitting, particularly a heavy tail distribution can generate very high values compared to the mode values and in the classical norms, this high values will contribute a lot to the total error and thus to the fitting results.

RESULTS

The parameters of the theoretical distributions are estimated by minimising (4) *i)* for all the drops of the measured drop spectrum and *ii)* only for drops with $D \geq D_{\text{threshold}}$. Then, the theoretical pdfs of the diameters are finally determined. Thus, for each fitting, the theoretical DSDs are easily computed by multiplying the retrieved pdf by n_c ; a graphical example is shown in Fig. 1, where the measured DSD (blue stars) and the retrieved DSD depicted as *i)* a green line and points and *ii)* a red line and points. In Fig. 1d, the gamma DSDs (eq.(2)) with the three parameters obtained by the method of moments (MM346 and MM012) are also plotted. The MM346, using higher moments, is more sensitive to the presence of larger drops, performing a sort of tail fitting, while MM012 can well represent the lower part of the spectra but it underestimates the $N(D)$ for larger drops. As expected, the DSD obtained from the entire spectrum represents the shape of the distribution better but could not adequately describe the upper part of the measured spectrum, decreasing more slowly.

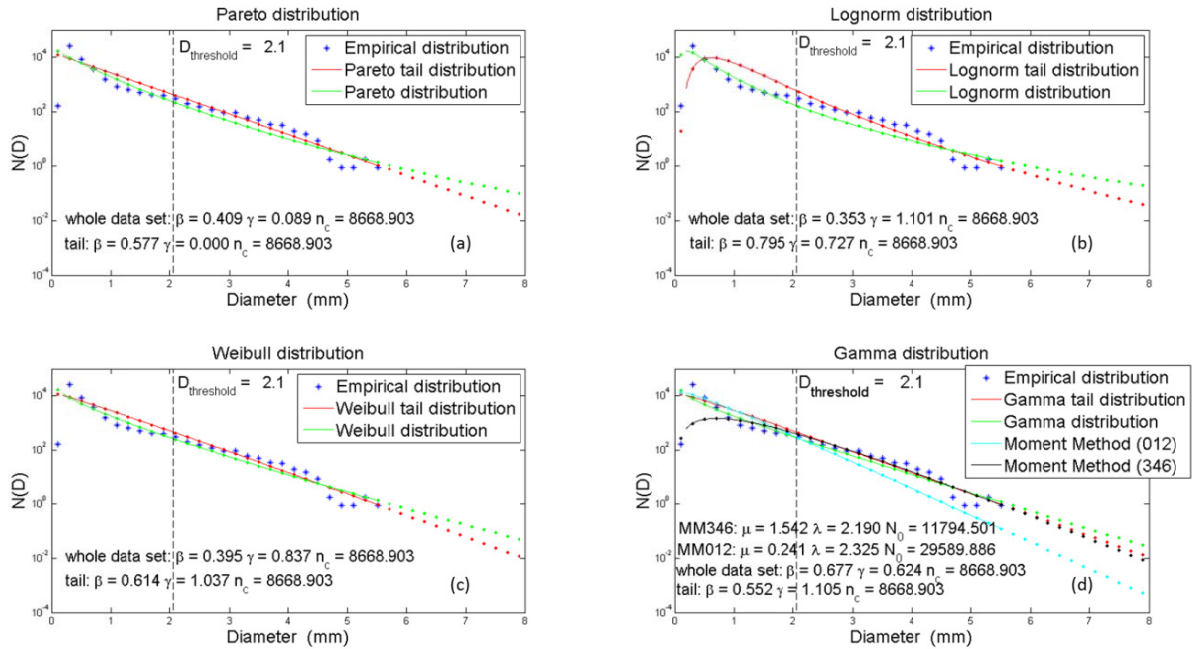


FIGURE 1. In each plot, the green line depicts a theoretical distribution fitted to the whole measured spectrum (blue stars), and the red line depicts the distribution fitted only to the large drops (blue stars right of the dashed line). Light blue and black lines are the gamma DSDs obtained using the method of moments (MM012 and MM346, respectively). The red, green, light blue and black points represent an extrapolation of the respective distributions.

Table 1 lists summary statistics of the norm $M1$ and of the parameters γ and β obtained by fitting only the large drops observed in this study. Results show that the shape parameter (γ) of the Pareto distribution is most of the time really low ($\gamma < 10^{-5}$), meaning that the distribution degenerates to the Exponential distribution, which is light-tailed and widely used to describe DSDs [1].

TABLE 1: Statistics from the fitting of the four distribution tails into the upper part of the DSDs

	Pareto			Lognormal			Weibull			Gamma		
	N1	β	γ	N1	β	γ	N1	β	γ	N1	β	γ
Min	0.006	0.151	2,02E-15	0.003	0.000	0.267	0.002	0.066	0.485	0.002	0.081	0.071
Mean	0.129	0.574	0,0088	0.036	1.011	0.640	0.029	0.898	1.399	0.029	0.396	3.176
Median	0.102	0.581	7,85E-10	0.023	1.009	0.603	0.021	0.891	1.357	0.021	0.368	2.539
Max	0.541	1.034	0,2921	0.649	2.349	6.619	0.293	2.235	3.220	0.296	1.340	21.066
Std	0.100	0.095	0,0346	0.043	0.312	0.323	0.027	0.305	0.391	0.027	0.180	2.649

According to our fitting methodology explained above, the theoretical distribution that gives the minimum values of the norm $N1(4)$ is the curve that has the best fit to the observational data. In Fig. 2, for each theoretical distribution, the percentages of 1-min spectra that are better fitted are shown. The comparisons are performed considering both the whole measured spectrum (Fig. 2a) and only the bigger drops (Figs. 2b and 2c). In Fig. 2a, there are the results obtained fitting the whole spectrum: the Weibull distribution is the best with a percentage of success equal to approximately 37%, and the Lognormal and the Gamma fit the measured spectrum better in approximately 30% of the time and the Pareto distribution is approximately 1%. Similar results are obtained fitting the whole spectrum and comparing the fitting only on the upper part of the spectra (Fig. 2b). In this condition, an increase of the percentage of success of the Weibull distribution (from 37% to 45%) is obtained, and the Pareto distribution is still the worst though with a slightly higher percentage of success. Finally, in Fig. 2c, the performance of the tail fitting is shown: 46% for Weibull, 39% for Lognormal, 15% for Gamma and less than 1% for Pareto. According to these percentages, the Weibull distribution is again the best. Moreover when the latter distribution is the best fit, the shape parameter (γ) is always greater than 1 (except once where $\gamma=0.985$) with a mean equal to 1.464; therefore the distribution with the lightest tail seems to be the one that fits the tail of the disdrometer-measured drop spectra better.

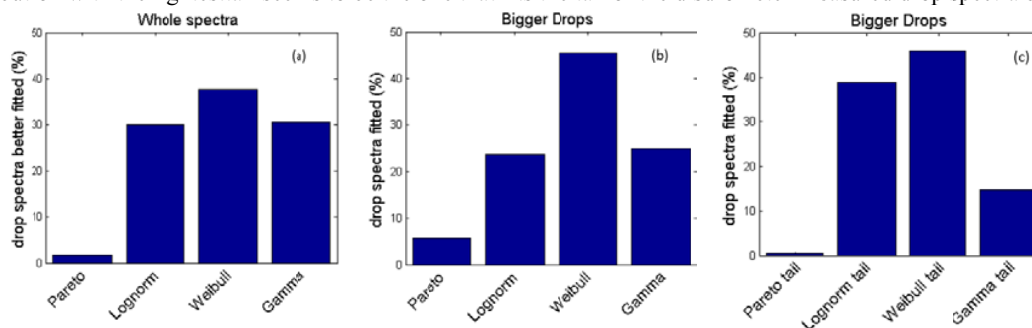


FIGURE 2. For each theoretical distribution the percentage of the 1-min spectra better fitted is reported considering both the entire spectrum (a) and tail (b and c). In (b), the theoretical EPF is obtained fitting the whole measured distribution, and in (c), the fitting is performed only in the tail. The distribution that better fits a given drop spectrum is the one with the minimum $N1$.

ACKNOWLEDGMENTS

Authors acknowledge International and Italian HyMeX SOP 1 coordination, NASA PMM (Dr. A. Hou and W. Petersen) for scientific cooperation and provision of instruments, and Department of Electronic Engineering, "Sapienza" University of Rome (Prof. F.S. Marzano) for scientific cooperation and instruments hosting.

REFERENCES

1. Marshall, J. S., and W. M. Palmer, *J. Meteorol.*, **9**, 327-332 (1948)
2. Sekine, M., and G. Lind, "Rain attenuation of centimetre, millimetre and submillimetre radio waves", in 12th European Microwave Conference Proceedings, Helsinki, Finland, 1982
3. Feingold, G., and Z. Levin, *J. Climate Appl. Meteor.*, **25**, 1346-1363 (1986)
4. Ulbrich, C., *J. Climate Appl. Meteor.*, **22**, 1764-1775 (1983)
5. Tokay, A. and Short, D. A., *J. Appl. Meteor.*, **35**, 355-371 (1996)
6. Handwerker, J., Winfried S., *J. Atmos. Oceanic Technol.*, **28**, 513-529 (2011)
7. Ulbrich, C. W., and Atlas D., *J. Appl. Meteor.*, **37**, 912-923 (1998)
8. Tokay, A., Petersen, W. A., Gatlin, P., and Wingo, M., *J. Atmos. Oceanic Technol.*, in press. (2013)
9. Villermaux E., Bossa B., *Nature Physics*, **5**, 697 - 702 (2009)
10. Schönhuber, M., G. Lammer, and W. L. Randeu, *Adv. Geosci.*, **10**, 85-90 (2007)
11. Gunn, R., and G. D. Kinzer, *J. Meteor.*, **6**, 243-248 (1949)
12. Tokay, A., Kruger, and W. Krajewski, *J. Appl. Meteor.*, **40**, 2083-2097 (2001)
13. Papalexioiu, S. P., Koutsoyiannis, D., Makropoulos, C., *Hydrol. Earth Syst. Sci.*, **17**, 851-862 (2013)
14. El Adlouni, S., Bobée, B., and Ouarda, T. B. M. J., *J. Hydrol.*, **355**, 16-33 (2008)